Supplementary Materials for

A Fundamental Analysis of Enhanced Cross–Coupling Catalytic Activity for Palladium Clusters on Graphene Supports

Y. Yang,[a] C. E Castano,[a] B. Frank Gupton,[a]*, A. C. Reber[b] and S. N. Khanna[b]*

Affiliations:

[a]Department of Chemical and Life Science Engineering, Virginia Commonwealth University Richmond, VA 23284

[b]Department of Physics, Virginia Commonwealth University, Richmond, VA 23284

*Correspondence to: bfgupton@vcu.edu (B. Frank Gupton), snkhanna@vcu.edu (S. N. Khanna)

Table of contents

S1 Materials and methods

Materials

Single layer Graphene oxide was purchased from Garphene Laboratories Inc. and used after purified. Rink amide MBHA resin (200-400 mesh, 0.07 mmol/g) was purchased from Che-IMPEX INT'L Inc.. Palladium nitrate (10 wt.% in 10 wt.% HNO_3, 99.999%) and hydrazine hydrate were obtained from Sigma Aldrich. 4-Iodo-benzonic acid, 4-Iodo-benzamide, potassium carbonate, phenlboronic acid, 1-hydroxybenzotriazole and N,N′-diisopropylcarbodiimide were also purchased from Aldrich and used as received.

Typical procedure for Suzuki reaction

Bromobenzene (50 mg, 0.32 mmol, 1 eq.) was dissolved in a mixture of 4 mL H_2O–EtOH (1 : 1) and placed in a 10 mL microwave tube. Phenyl boronic acid (47 mg, 0.382 mmol, 1.2 eq.), potassium carbonate (133 mg, 0.96 mmol, 3 eq.) was then added to the solution. 0.5 % Pd/G was then added, the tube was sealed, stirred and heated at 80 ℃ for 10 min under microwave irradiation (250 W, 2.45 MHz). After the reaction, the mixture was diluted with 10 mL of EtOH and test in GCMS/HPLC.

Leaching test

Prepare 4-Iodo-benzamide bound rink amide resin

Rink amide resin (1.0 g) was added to a 30 ml cartridge with 70μ frit. Dimethylformamide (DMF) 20 ml was then added to swell the resin for 30 min. Piperidine 20% was added to remove the protecting group. 4-Iodo-benzonic acid (1.04 g, 4.2 mmol), hydroxybenzotriazole (0.642 g, 4.2mmol) and diisopropylcarbodiimide (0.529

g, 4.2mmol) were premixed in CH_2Cl_2 (20ml) then added to the resin. The cartridge was capped and stirred for 6 hours. The CH_2Cl_2 was then removed. The resin was wash in dimethylformamide (3 × 15 ml), CH_2Cl_2 (3 × 15 ml) and methanol (3 × 15 ml) for 2 min each washing. The resin was dried in a vacuum for 24 hours at 0 ℃. The 4-Iodo-benzamide bound rink amide resin was then stored at 0 ℃ when not in use. To determine the 4-Iodo-benzamide loading, 100mg 4-Iodo-benzamide bound rink amide resin was added to 5ml DMF to swelling for 30 min in a 10 ml cartridge with 70μ frit. Trifluoroacetic acid (0.95 ml) and deionized H_2O (0.05 ml) was add to the resin after remove DMF. The cartridge was then capped and stirred for 4 hours. The solution was then collected and washed with DMF (2 × 5 ml) and CH_2Cl_2 (2 × 5 ml). All wash solutions were combined with first solution then run through HPLC (Water Acquity H class) and GC/MS (HP 6890 Series) versus internal standard. 4-Iodo-benzamide 0.102 g was yielded which correlate to 0.7 mmol/g loading resin.

Three phase test

100mg 4-Iodo-benzamide bound rink amide resin (0.07mmol 4-Iodo-benzamide) was added to 5ml DMF to swelling for 30 min in a 10 ml cartridge with 70μ frit. The DMF was then removed. Phenlboronic acid (24.5 mg, 0.22 mmol), K_2CO_3 (55.2 mg, 0.4 mmol), Pd/G catalyst 30% and swelled resin were added to 2 ml ethanol and H_2O (1:1) solution. The cartridge was capped and stirred for 20 hours at rt. The resin was then wash in dimethylformamide (3 × 2 ml), CH_2Cl_2 (3 × 2 ml) and methanol (3 × 2 ml) for 2 min each washing. Trifluoroacetic acid (0.95 ml) and deionized H_2O (0.05 ml) was add to the resin after wasing. The cartridge was then capped and stirred for 4 hours. The solution was then collected and washed with DMF (2 × 5 ml) and CH_2Cl_2 (2 × 5 ml). All wash

solutions were combined with first solution then run through HPLC versus internal standard.

S2 Structure and energy of Free Pd_n Cluster

Fig. S1

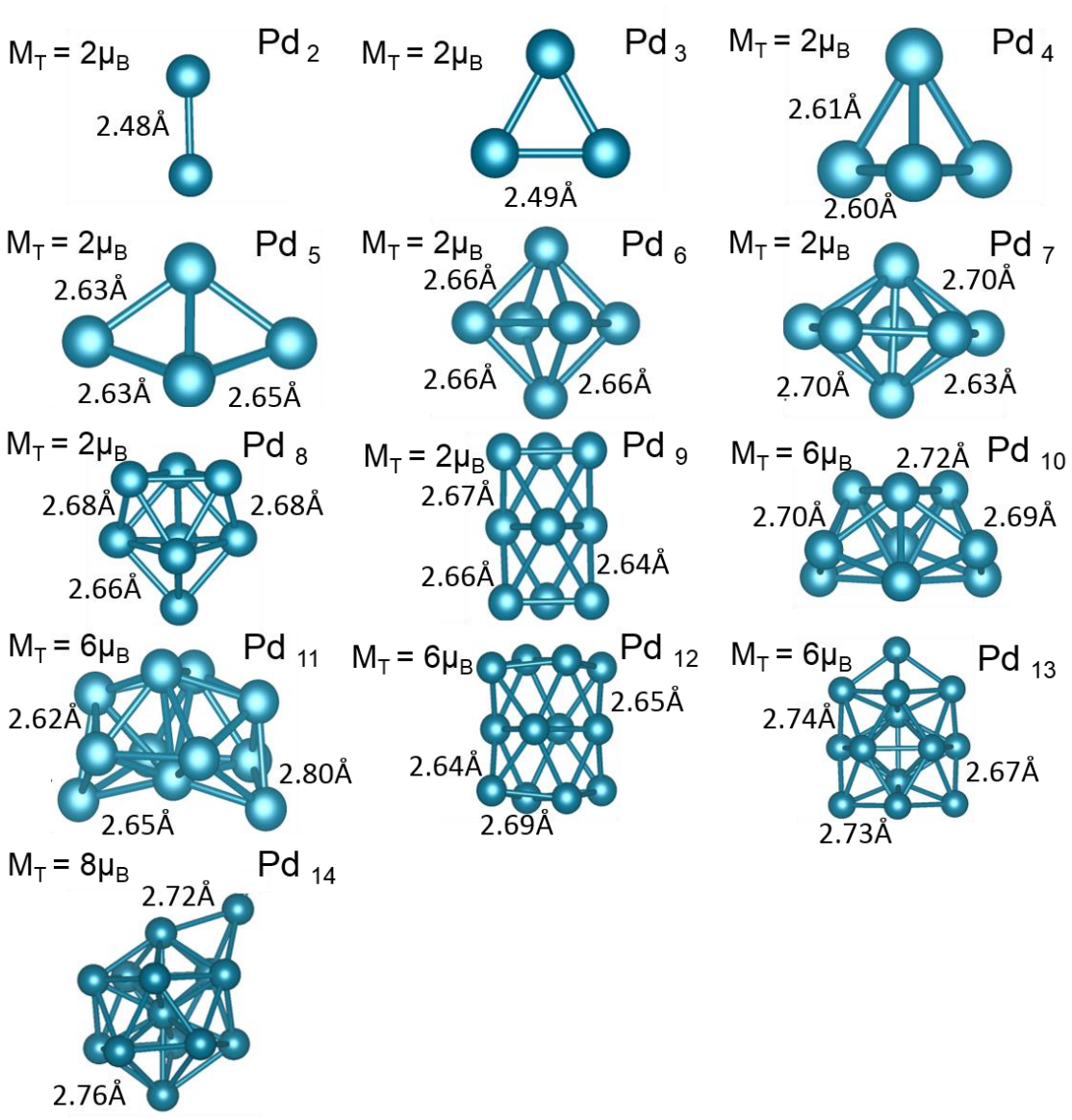

Fig. S1 The ground state atomic structures, magnetic moment and selected bond length of free $Pd_{2\text{-}14}$ clusters.

Table S1

Pd cluster	Avg. Binding energy (eV)	Spin multiplicity	Ionization potential (eV)
1	-	1	8.80
2	0.65	3	7.77
3	1.27	3	7.81
4	1.68	3	6.78
5	1.81	3	6.62
6	1.89	3	6.41
7	2.01	3	6.37
8	2.11	3	6.18
9	2.20	3	6.15
10	2.24	7	6.19
11	2.29	7	6.22
12	2.35	7	6.21
13	2.41	7	5.95
14	2.43	9	5.91

Table S1 Average binding energy, spin multiplicity and vertical ionization potential of $Pd_{1\text{-}13}$ cluster are listed.

We calculated the average binding energy (ABE) per atom using the expression

$$\text{Avg} = (nE(Pd) - E(Pd_n))/n$$

where $E(Pd_n)$ is the total energy of the cluster of n atoms, and E(Pd) is the atomic energy. We also calculated the vertical ionization potential (VIP)

$$\text{VIP} = E(Pd_n^+) - E(Pd_n)$$

as the difference in energy between the ground state of the neutral and that of the cation in the neutral ground state geometry.

Fig. S2

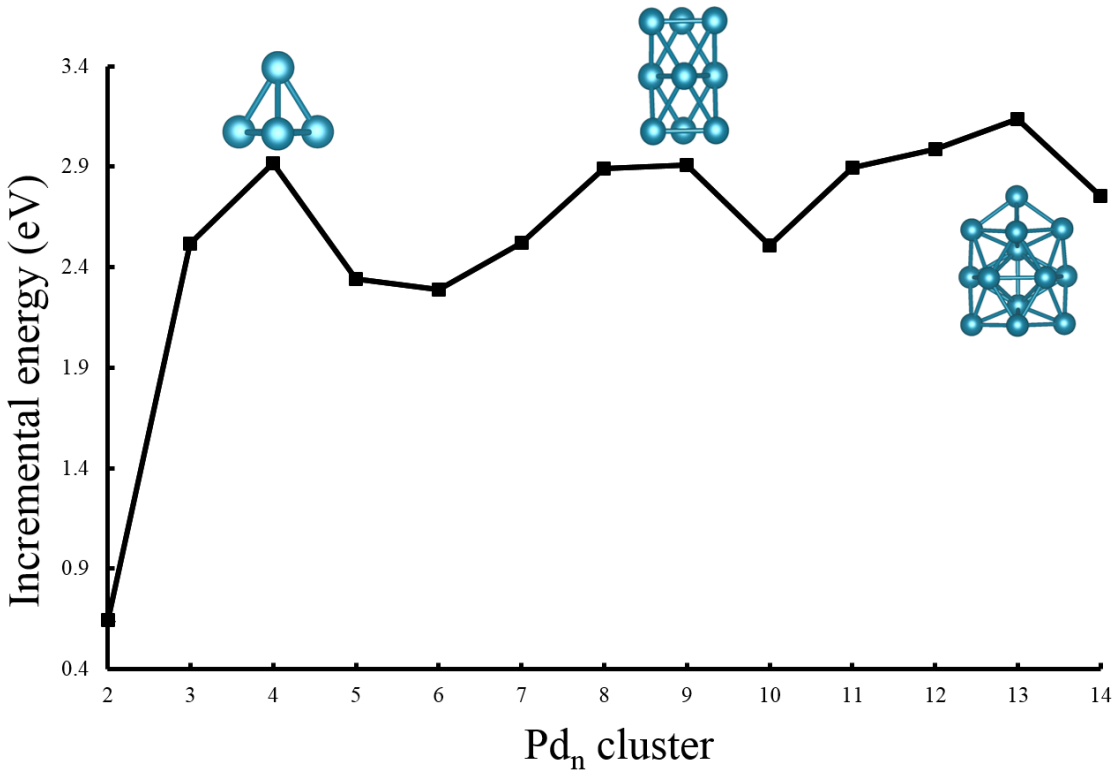

Fig. S2 Incremental binding energy of $Pd_{2\text{-}13}$ cluster indicates that Pd_4, Pd_9 and Pd_{13} show local maxima energy.

S3 Structure and energy of defected graphene

Fig. S3

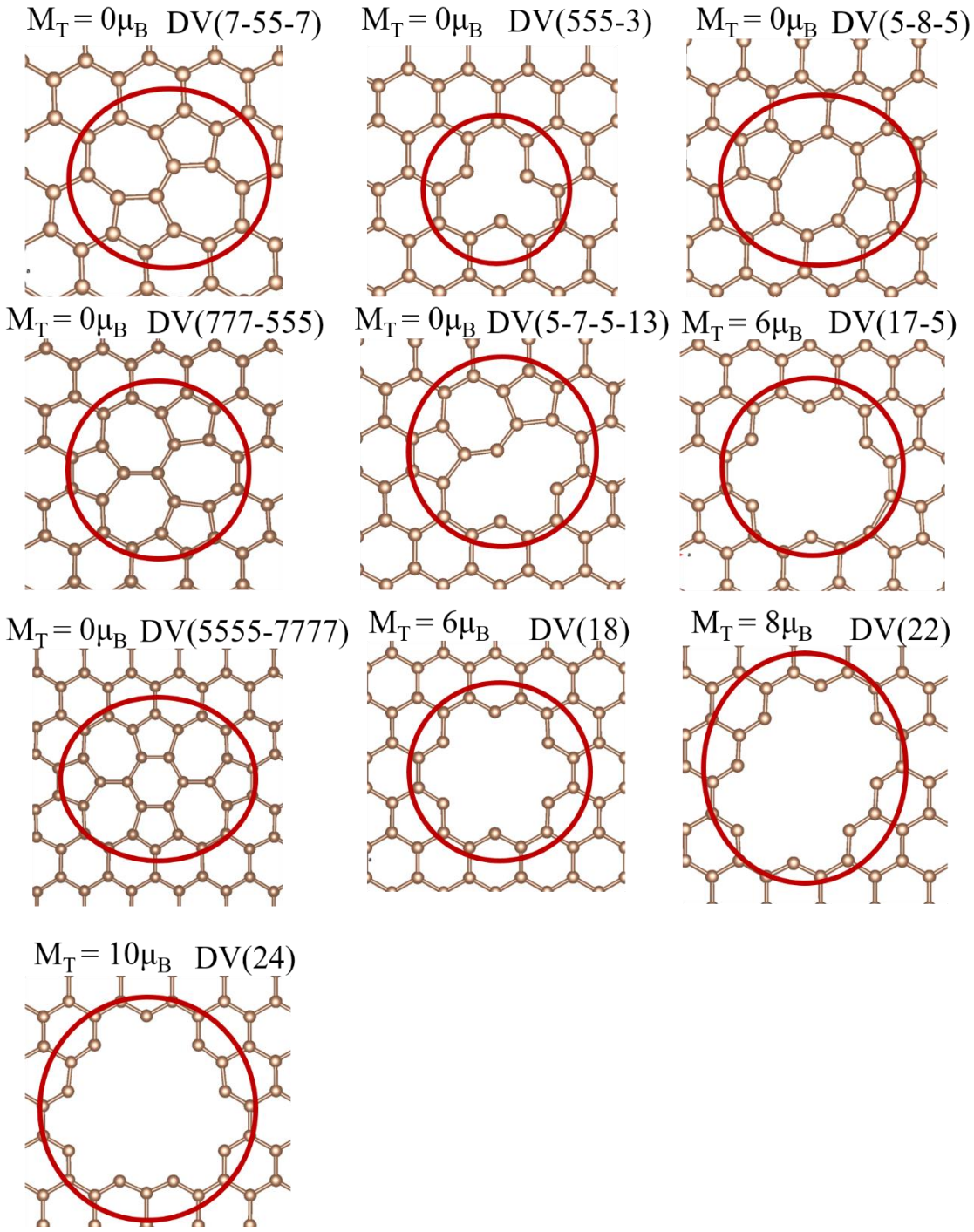

Fig. S3 Spin magnetic moment and the nature of the polygons around the defected site

Table S2

Defected graphene	Size of Vacancy (Num. of C)	Size of Vacancy (Å)	Defect energy (eV)	Spin multiplicity
DV(7-55-7)	0	3.2	5.11	1
DV(555-3)	1	4.4	17.12	1
DV(7777-5555)	2	3.2	25.82	1
DV(777-555)	2	3.2	26.17	1
DV(5-8-5)	2	5.0	26.36	1
DV(5-7-5-13)	3	5.5	40.97	1
DV(18)	6	6.7	72.97	7
DV(17-5)	7	7.0	83.67	7
DV(22)	10	8.6	115.97	9
DV(24)	13	9.0	148.56	11

Table S2 The nature and size of the defect and the associated spin multiplicity are listed. Defected site is shown according to the number of missing carbon and size in Angstrom. Defect energy is the energy difference between defected graphene sheet and pristine graphene sheet.

S4 Structure and energy of Pd_n cluster binding to defected graphene

Fig. S4

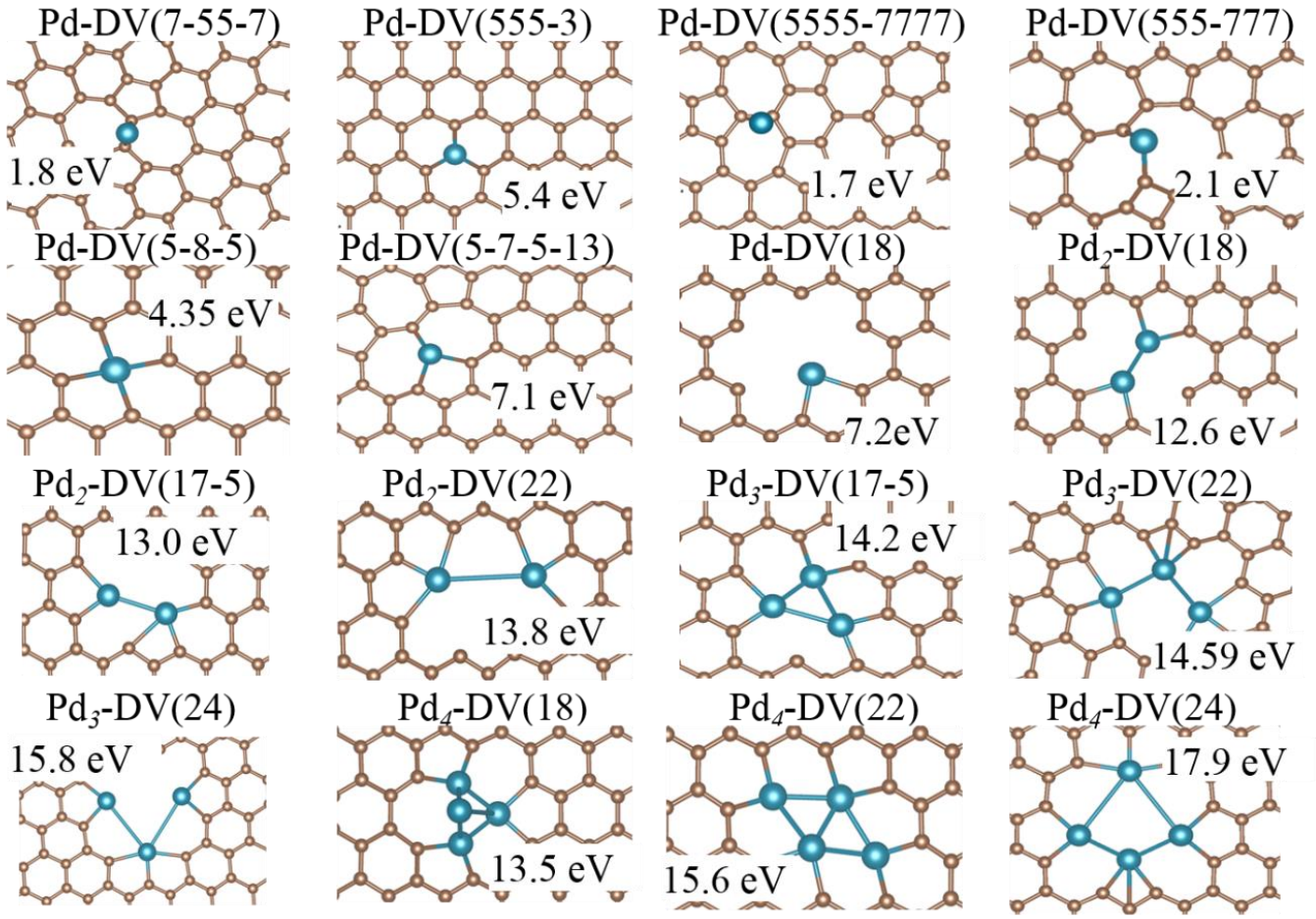

Fig. S4 $Pd_{1\text{-}5}$ bound to various size and structure of vacancy defected graphene.

Table S3

Pd-Defected graphene	Size of Vacancy (Num. of C)	Pd binding energy (eV)	Spin multiplicity
Pd-DV(7-55-5)	0	1.8	1
Pd-DV(555-3)	1	5.4	1
Pd-DV(5555-7777)	2	1.7	1
Pd-DV(777-555)	2	2.1	1
Pd-DV(5-8-5)	2	4.3	1
Pd-DV(5-7-5-13)	3	7.1	1
Pd-DV(18)	6	7.2	1
Pd_2-DV(18)	6	12.6	1
Pd_2-DV(17-5)	7	13.0	1
Pd_2-DV(22)	10	13.8	1
Pd_3-DV(17-5)	7	14.2	1
Pd_3-DV(22)	10	14.5	1
Pd_3-DV(24)	13	15.8	1
Pd_4-DV(18)	6	13.5	1
Pd_4-DV(22)	10	15.6	1
Pd_4-DV(24)	13	17.9	1

Table S3 The binding energy of $Pd_{1\text{-}4}$ bound to various sizes and structures of vacancy defected graphene are listed, along with the spin multiplicity.

S5 Structure energy and charge state of Pd_n (n=1-14) cluster binding to double vacancy defected graphene

Fig. S5

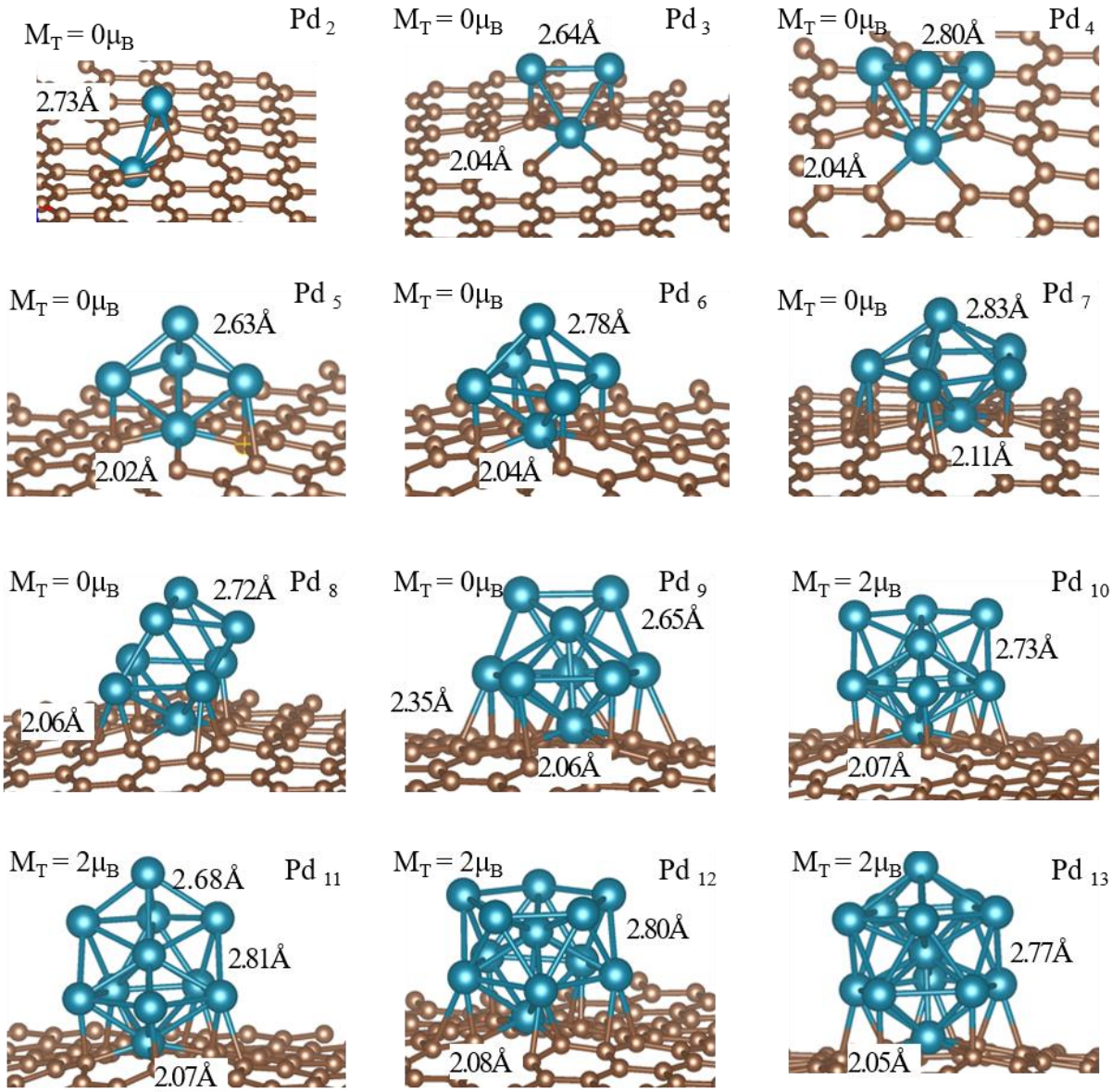

Fig. S5 Ground state geometries of Pd_{2-13} clusters on the double vacancy defected site are showed along with selected bond length and magnetic moment.

The ground state geometries are generally compact and in special cases, there are significant changes in the shape of the cluster. For example, for Pd_{13}, the ground state of the free cluster is a bi-layer structure while the ground state of the deposited species is a slightly distorted icosahedral structure. The change in structure can be related to the charging of the cluster and the effect of the support that can affect the ground state. Starting from Pd_4, the binding energy to the defect generally increases with cluster size and a Pd_{13} is bound by almost 7.4 eV compared to 5.4 eV for Pd_4. The increase in binding is accompanied by the larger charge donated to the surface and almost half the charge donated to the surface is derived from the Pd sites anchoring the cluster to the surface.

Table S4

Pd cluster	Avg. Pd Binding energy (eV)	Binding energy to defected graphene(eV)	Spin multiplicity	Charge donated to surface by Pd cluster	Charge donated to surface by anchor Pd
2	3.62	6.24	1	0.80	0.48
3	3.11	5.52	1	0.78	0.58
4	2.97	5.39	1	0.76	0.57
5	2.94	5.82	1	0.90	0.59
6	2.97	6.04	1	0.92	0.60
7	2.91	6.43	1	1.09	0.59
8	2.89	6.38	1	1.02	0.60
9	2.90	6.35	1	1.09	0.58
10	2.91	7.11	3	1.10	0.58
11	2.90	7.34	3	1.13	0.58
12	2.90	7.04	3	1.14	0.59
13	2.94	7.42	3	1.10	0.57
14	2.92	6.88	4	1.07	0.57

Table S4 Binding energy, spin multiplicity and charge state of Pd_{2-13} cluster are listed. Average binding energy is in the form of binding energy per Pd atom. The binding energy to the defect is the binding energy between the cluster defected graphene.

The Avg. Pd Binding energy (eV) was calculated as:

$$\text{Avg } E = (E(Pd_n/\text{graphene}) - nE(Pd) - E(\text{graphene}))/n$$

where $E(Pd_n/\text{graphene})$ is the total energy of the cluster and graphene, E(graphene) is the energy of graphene and E(Pd) is the atomic energy.

Table S5

Pd_{1-14}		Pd_1	Pd_2	Pd_3	Pd_4	Pd_5	Pd_6	Pd_7	Pd_8	Pd_9	Pd_{10}	Pd_{11}	Pd_{12}	Pd_{13}	Pd_{14}
Anchor (e^-)	Pd-1	9.46	9.51	9.42	9.42	9.51	9.39	9.41	9.39	9.41	9.41	9.41	9.41	9.42	9.43
Bottom layer (e^-)	Pd-2		9.67	9.91	9.86	9.83	9.89	9.89	9.82	9.87	9.82	9.82	9.82	9.86	9.92
	Pd-3			9.88	9.87	9.89	9.88	9.91	9.86	9.82	9.93	9.83	9.85	9.95	9.90
	Pd-4				10.07	9.82	9.88	9.84	9.90	9.84	9.85	9.86	9.85	9.88	9.83
	Pd-5					10.14	9.90	9.87	9.85	9.83	9.87	9.88	9.83	9.87	9.87
	Pd-6						10.10	9.85	10.01	9.91	9.97	9.89	9.97	9.90	9.84
Top layer (e^-)	Pd-7							10.10	10.04	10.08	10.05	9.97	9.97	10.00	9.96
	Pd-8								10.07	10.03	10.01	10.01	10.05	10.05	10.08
	Pd-9									10.07	10.07	10.07	10.04	10.04	10.05
	Pd-10										10.01	10.05	10.04	10.03	10.01
	Pd-11											10.01	10.04	10.06	10.00
	Pd-12												10.04	10.05	10.03
	Pd-13													10.05	10.07

Table S5 Individual Pd atom charge states in double vacancy defected graphene supported Pd_n clusters (n=1-14) are shown in the list. Anchor Pd is marked by large electrons transfer to graphene substrate. Bottom layer Pd atoms show slightly positive charge in some structure. Upper layer Pd, on the other hand, is neutral. Note that the charge on neutral Pd atom is 10 (e^-)

S6 Energy and charge state in oxidative addition reaction

Table S6

Pd cluster	Reactant E_b (eV)	Product E_b (eV)	Energy Gain (eV)	Br-C distance (Å)	Activation Energy(eV)
Pd_4	1.05	1.99	0.94	1.932	0.21
Pd_{13}	2.65	3.10	0.55	1.936	0.37
Pd_{14}	1.92	2.64	0.72	1.934	0.31
Pd_4/graphene	1.90	2.47	0.57	1.934	0.08
Pd_{13}/graphene	2.31	3.33	1.02	1.932	0.15
Pd_{14}/graphene	0.98	2.44	1.46	1.930	0.09

Table S6 The reagent and catalyst binding energy of the initial state and final state are listed as E_b. The activation energy of the Pd_4, $Pd_{13,}$ and Pd_{14} cluster is the energy difference between the initial bound state and the transition state.

Br-C bond Energy Eb:

Eb = E(Pd/g+BaBr)-E(Pd/g+Ba)-E(Br)

E(Pd/g+BaBr) is the total energy of the system when bromobenzoic acid is deposited on the surface of the catalyst.

Table S7

	Initial state(e^-)	Transition state(e^-)	Final state(e^-)
Pd	0.22	0.24	0.40
Benzoic acid	-0.13	-0.10	-0.05
Bromine	-0.08	-0.13	-0.35
Pd_4	0.17	0.20	0.65
Benzoic acid	-0.14	-0.10	-0.20
Bromine	-0.024	-0.10	-0.45
Pd_{13}	0.34	0.48	0.74
Benzoic acid	-0.27	-0.24	-0.38
Bromine	-0.064	-0.24	-0.36
Pd_{14}	0.16	0.31	0.59
Benzoic acid	-0.10	-0.10	-0.24
Bromine	-0.06	-0.20	-0.35

Table S7 The table lists the net Bader charge state of the Pd_n cluster, bromine atom and benzoic acid fragment when the 4-bromo-benzoic acid is in the initial state on the Pd_n, cluster, at the transition state, and at the final product. Note that in isolated 4-bromobenzoic acid, the charge on Br is -0.58 $e^-$and benzoic acid is 0.58 e^-.

Table S8

	Isolated catalyst(e^-)	Initial state(e^-)	Transition state(e^-)	Final state(e^-)
Pd_4	0.76	1.53	1.53	1.59
Anchor Pd	0.57	0.57	0.57	0.58
Benzoic acid	-	-0.29	-0.31	-0.23
Bromine	-	-0.06	-0.06	-0.44
Defected graphene	-0.76	-1.18	-1.15	-0.92
Pd_{13}	1.10	1.54	1.59	1.82
Anchor Pd	0.57	0.58	0.58	0.57
Benzoic acid	-	-0.30	-0.23	-0.33
Bromine	-	-0.07	-0.22	-0.37
Defected graphene	-1.10	-1.16	-1.15	-1.12
Pd_{14}	1.07	1.24	1.21	1.75
Anchor Pd	0.57	0.57	0.57	0.57
Benzoic acid	-	-0.09	-0.05	-0.29
Bromine	-	-0.07	-0.09	-0.40
Defected graphene	-1.07	-1.08	-1.07	-1.07

Table S8 The table lists the net Bader charge state of the Pd_n cluster not including the anchor atom, the Pd anchor atom, the bromine atom, the benzoic acid fragment, and the defected graphene sheet when the 4-bromo-benzoic acid is in the initial state on the Pd_n, cluster, at the transition state, and at the final product.

S7 Structure and energy of bromine absorption

Fig. S6

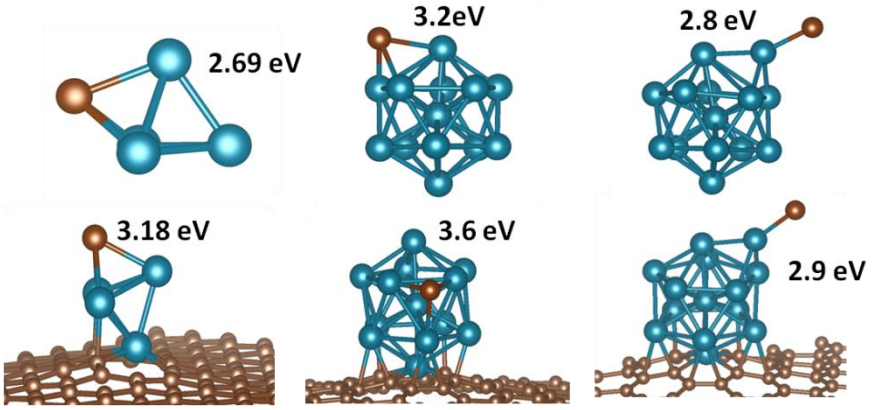

Fig. S6 Ground state structure of absorbed Br atom on free Pd_4, Pd_{13}, Pd_{14} cluster and graphene supported Pd_4, Pd_{13}, and Pd_{14} cluster.

Table S9

Pd cluster	Br Binding energy(eV)	Charge donated to Br
Pd_4	2.69	0.29
Pd_{13}	3.20	0.30
Pd_{14}	2.84	0.39
Pd_4-graphene	3.18	0.36
Pd_{13}-graphene	3.60	0.35
Pd_{14}-graphene	2.91	0.39

Table S9 Bromine adsorption energy and charge transfer of free and supported Pd_4, Pd_{13}, and Pd_{14} cluster.

S8 Density of state of the complexes at transition state

Fig. S7

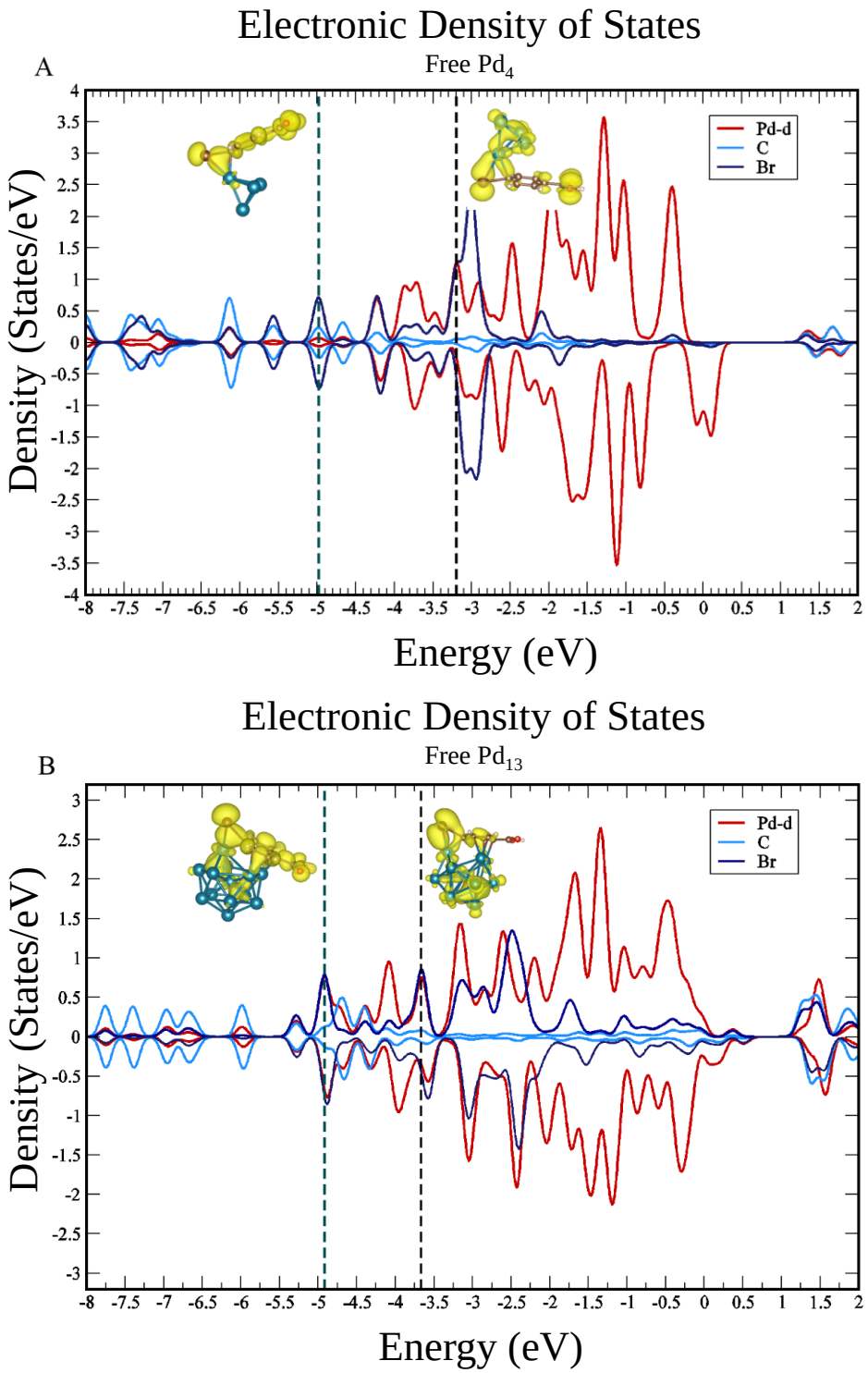

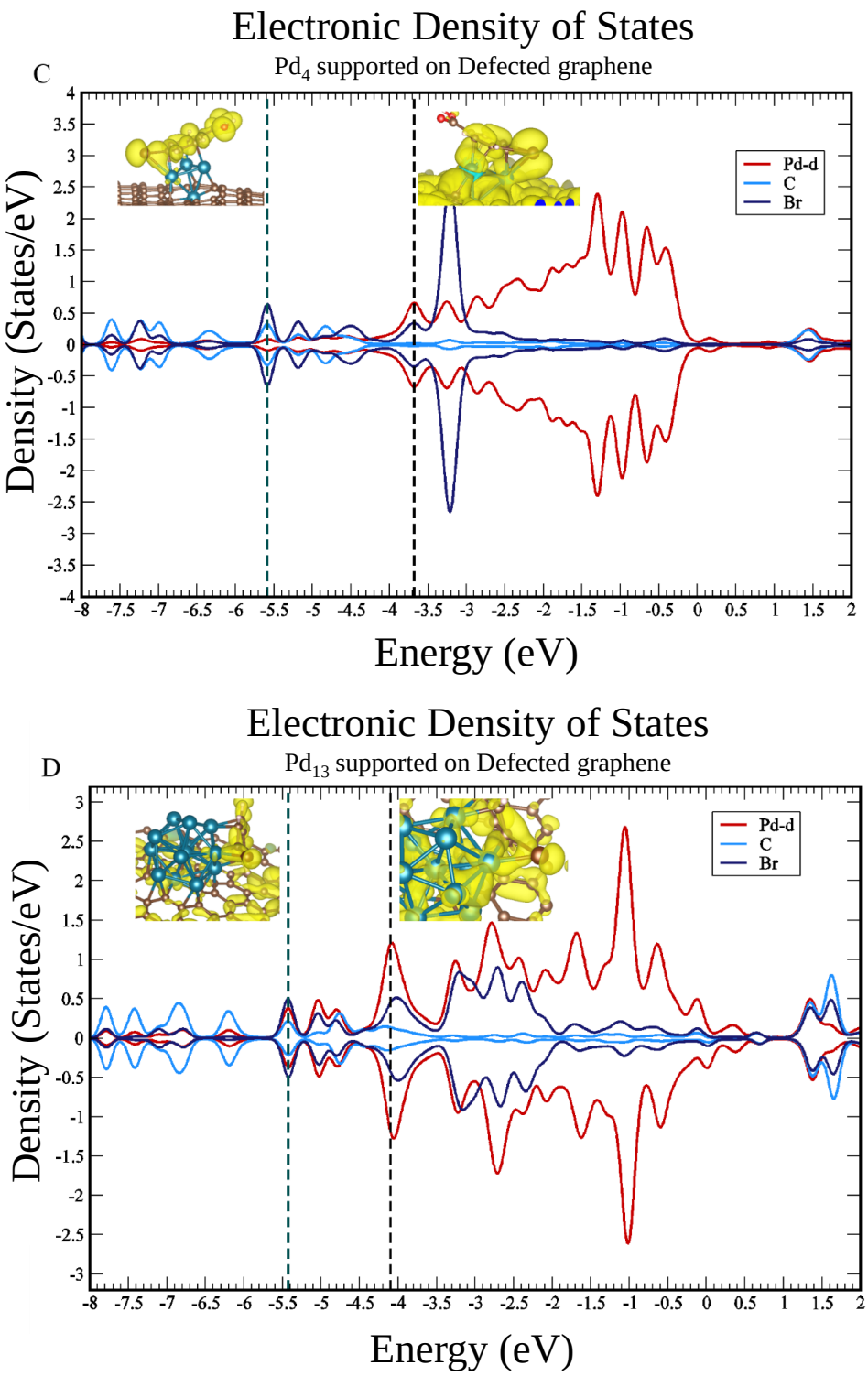

Fig. S7. A, B, C and **D** shows the 4d Pd atom at the active site, C, and Br orbital electron density of states of the Pd atom at the active site at the transition state of free Pd_4, Pd_{13} and supported Pd_4 and Pd_{13} respectively in oxidative addition reaction. Both the bonding and antibonding state are shifted left by 0.5eV after deposit the Pd_4 and Pd_{13} cluster on defected graphene.

S9 Energy and charge analysis in oxidative addition reaction

Table S10

	Initial state		Transition state			Final state	
	Br-C binding energy (eV)	BA-Pd binding energy (eV)	Bonding state energy level (eV)	Antibonding state energy level (eV)	Charge transfer enhance by supported (%)	Br-Pd binding energy (eV)	BA-Pd binding energy (eV)
Free 4-bromobenzoic acid	4.11	-	-	-	-	-	-
Pd_4	3.08	2.04	-5.0	-3.2	-	3.04	3.19
Pd_4/graphene	2.73	3.41	-4.9	-.3.7	47.6	3.52	3.20
Pd_{13}	3.01	3.89	-5.6	-3.6	-	3.54	3.89
Pd_{13}/graphene	2.66	3.91	-5.4	-4.1	20.0	3.78	3.91

Table S10 The Br-C bonding energy, and the benzoic acid binding energy at the initial (complexes) state are shown. At the transition state, the energy of the bonding and antibonding orbital that activates the Br-C bond are listed, as is the charge transfer enhancement that is found by comparing the transition state structure with and without the defected graphene support. At the final state, the binding energy of Br, and benzoic acid are shown.

S10 Catalyst particle size distribution and survey scan by x-ray photoelectron spectroscopy

Fig. S8

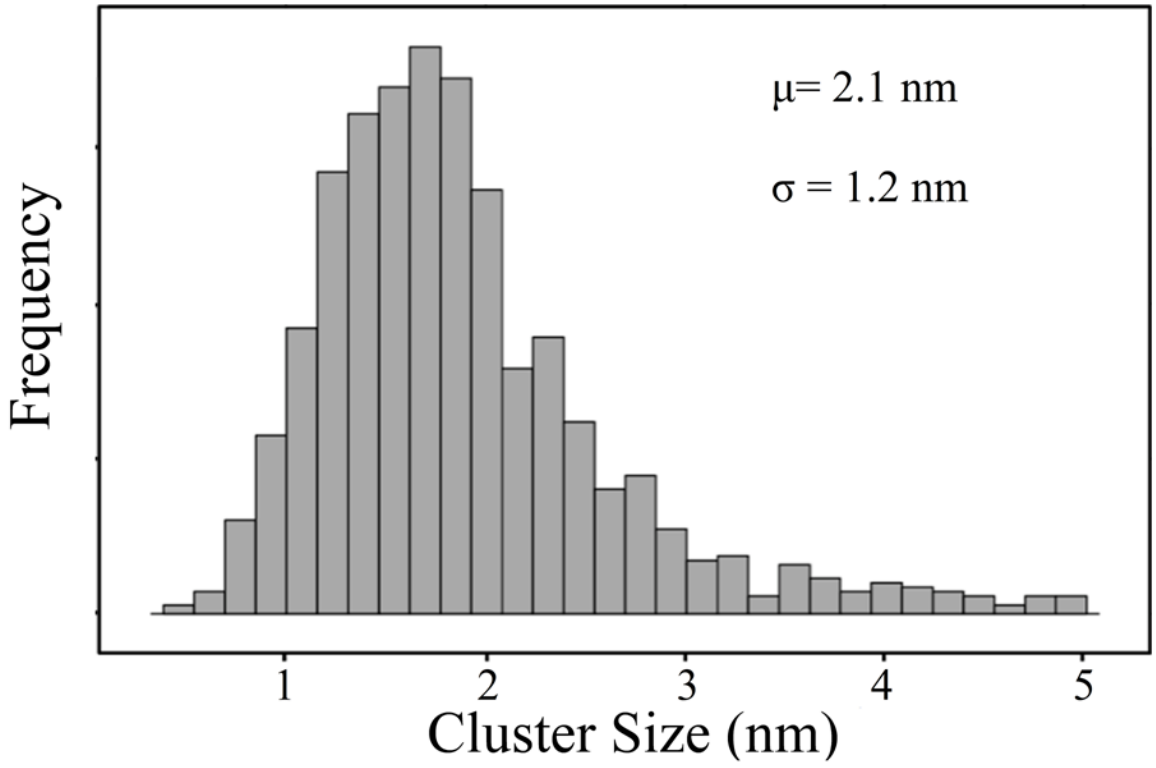

Fig. S8 Pd/G nanoparticle distribution counted throguh TEM image shows average size of Pd nanoparticle is 2.1 nm with standard deviation 1.2 nm. Small clusters, size less than 1 nm, exist on the surface as we showed in the theoretical study.

Fig S9

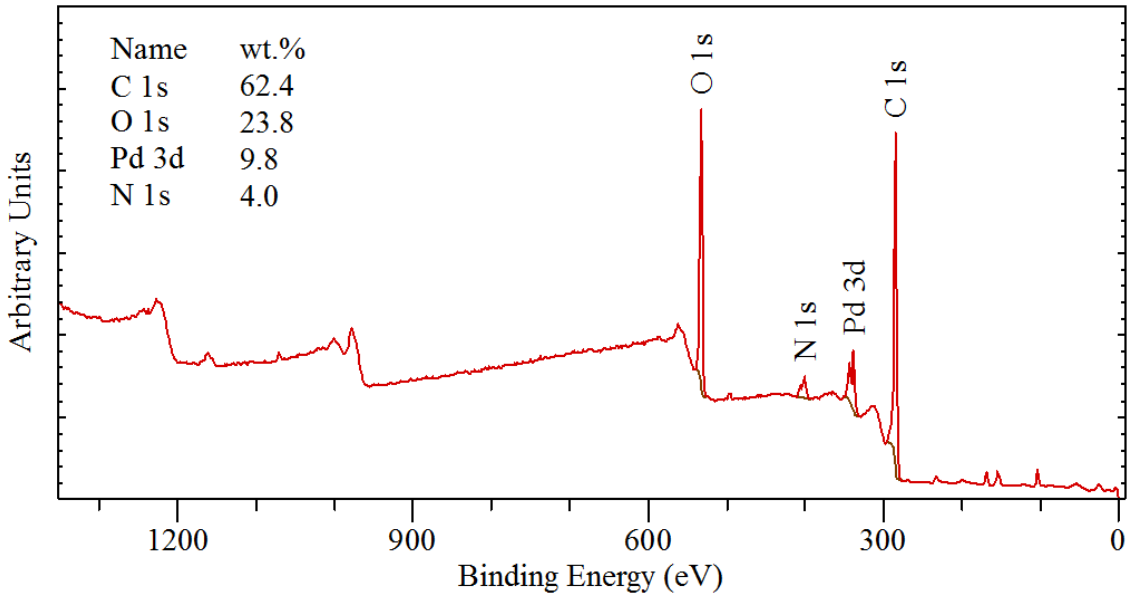

Fig S9. Elemental analysis on the surface of Pd/G catalyst measured by x-ray photoelectron spectroscopy.

S11 Control experiments Suzuki reaction

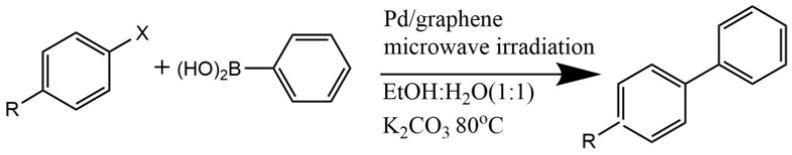

Entry	Aryl Halide	Conversion[a]
1	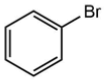	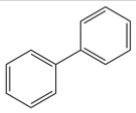 100%
2	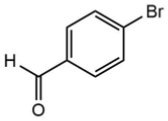	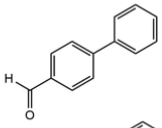 100%
3[b,c]	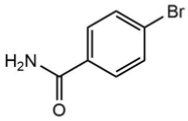	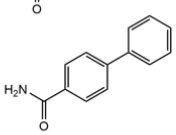 100%
4		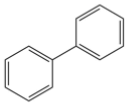 100%
5	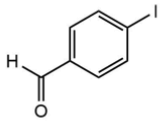	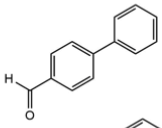 100%
6[b,c]	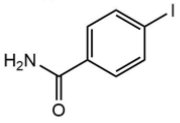	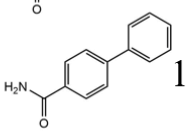 100%

a, Conversion confirmed by GCMS and HPLC. *b,* Similar conversion could be achieved by using $Pd(OAc)_2/PPh_3$ Catalyst. *c,* Similar conversion could be achieved by running reaction in 25 ℃ in 1 hour.

S12 Different reaction condition for three phase test

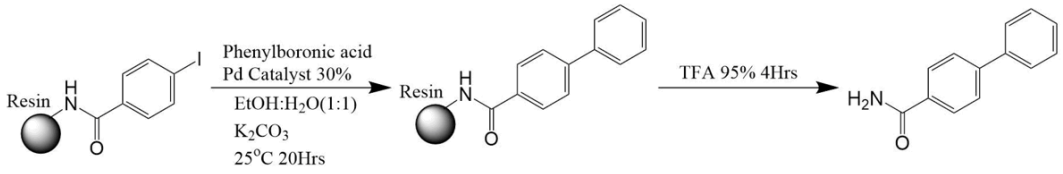

Resin bounded aryl halide	Pd Catalyst	Reaction temperature	Running time (Hour)	Conversion
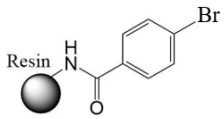	Pd/graphene	80°C[a]	2	<1%
	$Pd(OAc)_2/PPh_3$	80°C[a]	2	29%[b]
	Pd/graphene	25°C	20	<1%
	$Pd(OAc)_2/PPh_3$	25°C	20	45%
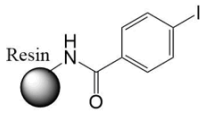	Pd/graphene	80°C[a]	2	<1%
	$Pd(OAc)_2/PPh_3$	80°C[a]	2	33%
	Pd/graphene	25°C	20	<1%
	$Pd(OAc)_2/PPh_3$	25°C	20	60%

a, Reaction was heated using microwave irradiation. *b,* Conversion achieved 26% after 30mins.